# Optical bistability and pulsating behaviour in Silicon-On-Insulator ring resonator structures.

**G. Priem, P. Dumon, W. Bogaerts, D. Van Thourhout, G. Morthier, and R. Baets**

*Ghent University - IMEC, Department of Information Technology (INTEC)*
*Sint-Pietersnieuwstraat 41, 9000 Gent, BELGIUM*

*gino.priem@ugent.be*

**Abstract:** We demonstrate optical bistability in a Silicon-On-Insulator two-bus ring resonator with input powers as low as $0.3mW$. We evaluate the importance of the different nonlinear contributions and derive time constants for carrier and thermal relaxation effects. In some cases, we also observe pulsation due to interaction between the dominant nonlinear effects. Such a behaviour may be problematic for possible memory and switching operations. Alternatively, it could be used for (tunable) pulse generation.



**OCIS codes:** (190.4390) Nonlinear optics, integrated optics; (190.1450) Bistability; (190.3100) Instabilities and chaos

## References and links

1. W. Bogaerts, R. Baets, P. Dumon, V. Wiaux, S. Beckx, D. Taillaert, B. Luyssaert, J. Van Campenhout, P. Bienstman and D. Van Thourhout, "Nanophotonic waveguides in Silicon-on-Insulator fabricated with CMOS Technology," IEEE J. Lightwave Technol. **23,** 401–412 (2005).
2. D. Taillaert, P. Bienstman and R. Baets, "Compact efficient broadband grating coupler for silicon-on-insulator waveguides," Opt. Lett. **29,** 2749–2751 (2004).
3. V. Almeida and M. Lipson, "Optical bistability on a silicon chip," Opt. Lett. **29,** 2387–2389 (2004).
4. P. Barclay, K. Srinivasan and O. Painter, "Nonlinear response of silicon photonic crystal microresonators excited via an integrated waveguide and fiber taper," Opt. Express **13,** 801–820 (2005), http://www.opticsexpress.org/abstract.cfm?URI=OPEX-13-3-801.
5. M. Notomi, A. Shinya, S. Mitsugi, G. Kira, E. Kuramochi and T. Tanabe, "Optical bistable switching action of Si high-Q photonic-crystal nanocavities," Opt. Express **13,** 2678–2687 (2005), http://www.opticsexpress.org/abstract.cfm?URI=OPEX-13-7-2678.
6. G. Priem, P. Bienstman, G. Morthier and R. Baets, "Resonator-based all-optical Kerr-nonlinear phase shifting: design and limitations," J. Appl. Phys. **97,** 023104 (2005).
7. A. Melloni, F. Morichetti and M. Martinelli, "Linear and nonlinear pulse propagation in coupled resonator slow-wave optical structures," Opt. Quantum Electron. **35,** 365–379 (2003).
8. T.K. Liang and H.K. Tsang, "Role of free carriers from two-photon absorption in Raman amplification in silicon-on-insulator waveguides," Appl. Phys. Lett. **84**, 2745–2747 (2004).
9. R. Claps, V. Raghunathan, D. Dimitropoulos and B. Jalali, "Influence of nonlinear absorption on Raman amplification in silicon waveguides," Opt. Express **12**, 2774-2780 (2004), http://www.opticsexpress.org/abstract.cfm?URI=OPEX-12-12-2774.
10. D. Dimitropoulos, R. Jhaveri, R. Claps, J. Woo and B. Jalali, "Lifetime of photogenerated carriers in silicon-on-insulator rib waveguides," Appl. Phys. Lett. **86**, 071115 (2005).
11. H. Gibbs, *Optical bistability: controlling light with light* (Academic, Orlando, 1985).

## 1. Introduction

Photonic wire structures fabricated in high contrast systems such as Silicon-on-Insulator (SOI) allow strong transverse confinement of light within submicron dimensions. This optical con-

#8922 - $15.00 USD Received 27 September 2005; revised 8 November 2005; accepted 8 November 2005

finement can even be further enhanced in the longitudinal direction by using resonant structures such as ring resonators and photonic crystal (PhC) nanocavities, in which the propagation of the light pulse is slowed down. Such structures with high confinement are of great interest for nonlinear optics, as they allow nonlinear interaction with relatively low power levels.

In the Silicon system - for which the telecom wavelength $\lambda = 1.55\mu m$ is situated above half the band gap - this nonlinear picture is quite complex. It can be summarized as follows (Fig. 1): when light enters in the Silicon material, it can be absorbed through two-photon absorption (TPA) and results in a change in the refractive index effect proportional to the light intensity (Kerr effect). Through the TPA process, free carriers are excited which result in additional absorption (Free Carrier Absorption, FCA) and an associated index change (Free Carrier Dispersion, FCD). After a while, these carriers will recombine and in the case of submicron structures such as photonic wires, this is mainly due to surface recombination. This interband relaxation together with the intraband relaxation effects from carriers created due to TPA and FCA will lead to phonon creation, resulting in heating of the structure and giving rise to thermal expansion and a thermal refractive index change. Due to conduction and convection, the structure finally cools down to a steady-state temperature.

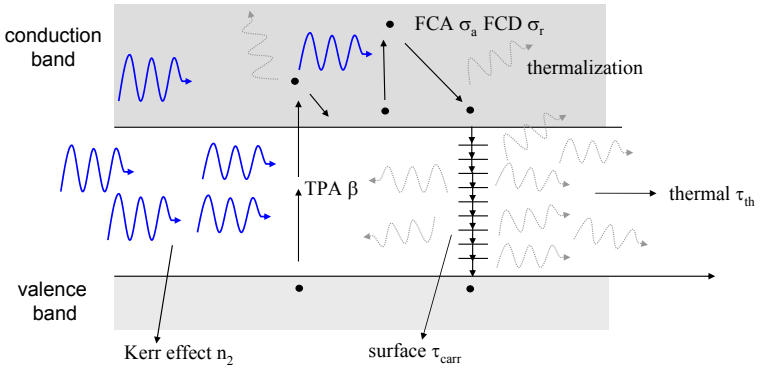


Fig. 1. Physical picture of the nonlinear interactions in Silicon for wavelengths around half the band gap.

In this paper, we evaluate the importance of the different nonlinear contributions for ultra-small two-bus ring resonators and derive time constants for carrier and thermal relaxation. We demonstrate optical bistability for input powers as low as $0.277mW$. We also observe pulsation due to interaction between the dominant nonlinear effects.

## 2. Design and fabrication

Resonator structures were created on 200*mm* SOI wafers with a thickness of the Silicon layer of 220*nm* and a burried oxide of $1\mu m$. A deep UV lithography stepper with a 248*nm* illumination wavelength is used to define the patterns in the resist. A dry etching process then transfers the patterns into the Silicon layer. A detailed overview of the processing steps can be found in [1]. The processes are essentially CMOS processes, characterized and adapted for the fabrication of photonic circuits, which enforces quite different technological boundary conditions. An example of an obtained resonator structure is shown in Fig. 2.

To couple the light from fiber to the input waveguide of the resonators, grating couplers were used with a peak efficieny of $\approx 25\%$ [2]. The resonator structure used for the experiments in this paper has a radius of $4\mu m$ and a wire width of approximately 540*nm*.

#8922 - $15.00 USD Received 27 September 2005; revised 8 November 2005; accepted 8 November 2005

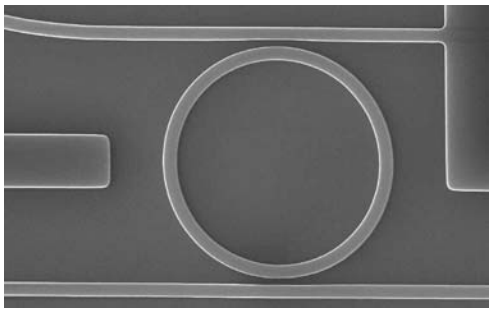

Fig. 2. Example of a ring resonator structure fabricated through deep UV lithography.

## 3. Experimental results

### *3.1. Pass and drop in the linear regime*

The normalized pass and drop spectra for the measured structure are shown in Fig. 3(a). The measured free spectral range (FSR) is 21.25*nm*. From detailed measurements around the reso-

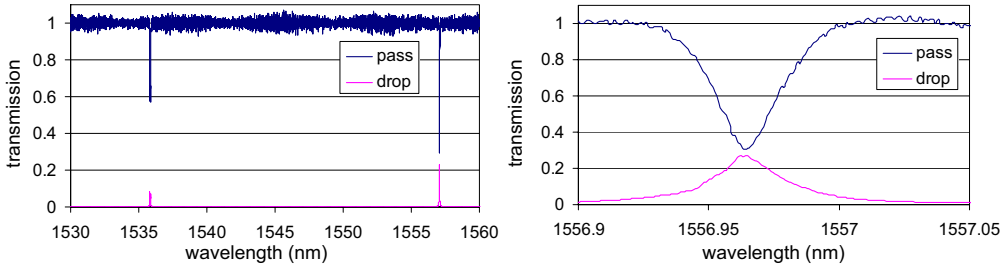


Fig. 3. (a) Normalized transmission of the pass and the drop port in the linear regime. (b) Detailed measurement around the resonance wavelength $\lambda_c = 1556.97nm$

nance wavelength at $\lambda_c = 1556.97nm$ (Fig. 3(b)), a resonance bandwidth $\Delta\lambda_{BW}$ $0.025nm$ was derived, corresponding to a Q-factor of $\approx 62500$. The resonance transmission of the drop port at this wavelength is about 27%.

### *3.2. Transmission in the nonlinear regime*

For the nonlinear measurements, the input power was increased from $0.069mW$ in steps of $3dB$ and from $0.277mW$ on in steps of $1.5dB$. The results together with the linear pass and drop spectra are shown in Fig. 4.

As can be seen in Fig. 4, bistability is obtained for input powers as low as $0.277mW$. Only the upper arm of the bistable solutions is shown, because of sweeping limitations of our measurement setup. This value is the lowest reported for ring resonator structures so far [3] and of the same magnitude as the results obtained with PhC nanocavities [4, 5]. However, note that the latter are standing-wave resonators, which have the benefit of better nonlinear interaction due to the presence of a contrapropagating wave inside the cavity (respectively $3\times$, $10\times$ and $35\times$ higher for third-, fifth- and seventh-order nonlinear effect [6, 7]).

#8922 - $15.00 USD Received 27 September 2005; revised 8 November 2005; accepted 8 November 2005

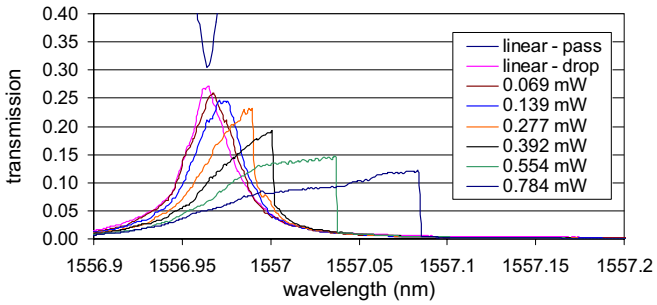


Fig. 4. Normalized transmission of the drop port for different input powers. The linear pass and drop transmissions are indicated as reference. Bistability is obtained for powers equal and above $0.277mW$

## 4. Discussion

From the decrease in the resonance transmission $T_{max}$ of the drop port and the shift of the resonance wavelength $\Delta\lambda$, information can be derived concerning the strength of the different nonlinear effects and the carrier and thermal relaxation time constants. To do this, $T_{max}$ and $\Delta\lambda$ are plotted as a function of the power inside the cavity in Fig. 5. These experimental results

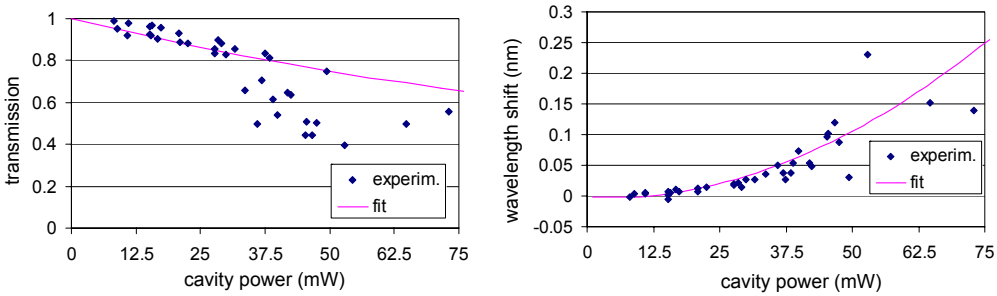


Fig. 5. (a) Nonlinear resonance transmission $T_{max}$ and (b) resonance shift $\Delta\lambda$ at the drop port as a function of the cavity power.

were fitted using an approach similar to the one described in [4]. From this, a carrier relaxation constant of $\tau_{carr} \approx \frac{5.3\times10^7}{N}s$ with $N[cm^{-3}]$ the carrier density and a thermal relaxation constant of $\tau_{th} \approx 65ns$ were derived. These relaxation times are in close agreement with the results obtained in [8, 9, 10, 4, 5]. The different nonlinear contributions to the refractive index change inside the cavity, which are responsible for the shift of the resonance wavelength are plotted in Fig. 6. Thermal effects are clearly dominant, but also the free-carrier dispersion effect is important. Three thermal contributions can be distinguished. Contributions due to TPA and FCA were already discussed in the introduction. The linear thermal refractive index change is required to obtain full agreement with the experimental results [4]. This temperature change can be explained through the presence of surface state absorption at the Silicon-Silica interface. A surface state absorption coefficient of $0.11dB/mm$ was derived.

Note the difference in Fig. 5 between the experimental results and the theoretical fit for higher power levels. This difference can be explained by the fact that for higher cavity powers, the resonator does not achieve a stable or bistable state, but instead starts to exhibit quasi-periodical pulsations. This behaviour originates from the fact that the two dominating nonlinear refractive index effects - the FCD effect and the associated thermal refractive index change - have opposite

#8922 - $15.00 USD Received 27 September 2005; revised 8 November 2005; accepted 8 November 2005

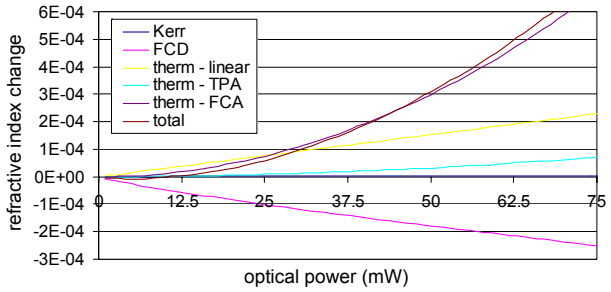


Fig. 6. Different nonlinear contributions to the refractive index change inside the ring resonator as function of the cavity power.

signs and different time constants. This can be qualitatively understood as a circling around the bistability loop [11]. The quasi-periodic nature is due to amplifier noise and laser fluctuations. As a result, the measured $T_{max}$ do not anymore correspond to a (bi)stable solution, but instead to a time-averaged transmission value of the quasi-periodical pulsation.

Due to this quasi-periodicity, the presence of these pulsations could not be verified directly by means of an oscilloscope. It was however done indirectly by measuring the standard deviation of the obtained output signal. This is shown in Fig. 7 for an input power of $0.76mW$. We clearly

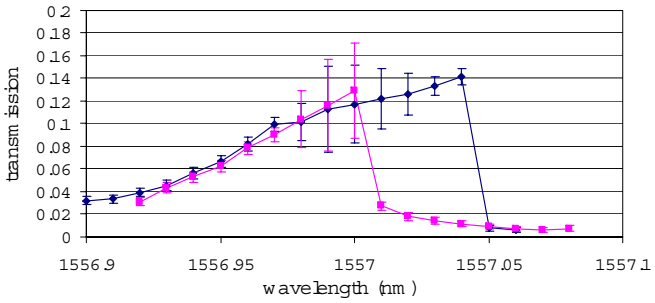


Fig. 7. Normalized average transmission and standard deviation at the drop port for an input power of $0.76mW$. The blue curve corresponds to a (manual) wavelength sweep from low to high, the violet curve from high to low.

see that the upper 'bistable' and even part of the 'stable' arm are in fact not stable, indicating the pulsating behaviour. In addition, note that the standard deviation is wavelength dependent: simulations have shown that both the pulse length and period change with wavelength and power of the input signal. This would make tunable pulse generation possible. A more detailed study of this effect will be published elsewhere.

## 5. Conclusion

We demonstrated optical bistability in a Silicon-On-Insulator two-bus ring resonator with input powers of only about $0.3mW$. Taking into account the higher nonlinear interaction in standing-wave structures, these results are comparable with the best results obtained with PhC resonators. Free carrier dispersion and carrier-related thermal refractive index change were identified as the dominant nonlinear contributions. A carrier relaxation constant of $\tau_{carr} \approx \frac{5.3\times10^7}{N}s$ with $N[cm^{-3}]$ the carrier density and a thermal relaxation constant of $\tau_{th} \approx 65ns$ were derived, al-

#8922 - $15.00 USD Received 27 September 2005; revised 8 November 2005; accepted 8 November 2005

lowing different nonlinear applications such as carrier-based optical switching (timescale $\propto 1ns$ for typical carrier densities of $N = 10^{16} - 10^{17} cm^{-3}$) and thermal bistable switching and memory operation (timescale $\propto 100ns$).

For higher input powers, we also observed pulsation due to interaction between these two dominant nonlinear effects. This can be understood as a circling around the (bistable) hysteresis curve. Such a behaviour may be problematic for the stability of thermal memory and switching operation. On the positive side, it could be used for tunable pulse generation: optimization of the input power and/or wavelength makes it possible to change both the pulse length and the pulse period.

**Acknowledgment**

This work was supported by the EU through the Network of Excellence ePIXnet. Part of this work has been performed in the context of the Belgian IAP PHOTON Network (IAP V/18).

Gino Priem and Wim Bogaerts acknowledge the Flemish Fund for Scientific Research (FWO-Vlaanderen) for financial support. Pieter Dumon thanks the Institute for the Promotion of Innovation through Science and Technology in Flanders (IWT-Vlaanderen) for a scholarship.

#8922 - $15.00 USD Received 27 September 2005; revised 8 November 2005; accepted 8 November 2005